We are IntechOpen, the world's leading publisher of Open Access books Built by scientists, for scientists

6,900
Open access books available

186,000
International authors and editors

200M
Downloads

Our authors are among the

154
Countries delivered to

TOP 1%
most cited scientists

12.2%
Contributors from top 500 universities

WEB OF SCIENCE™

Selection of our books indexed in the Book Citation Index in Web of Science™ Core Collection (BKCI)

Interested in publishing with us?
Contact book.department@intechopen.com

Numbers displayed above are based on latest data collected.
For more information visit www.intechopen.com

4

Application of Electron Beam Treatment in Polycrystalline Silicon Films Manufacture for Solar Cell

L. Fu
College of Materials Science, Northwestern Polytechnical University, Xian, State Key Laboratory of Solidification Processing P. R. China

1. Introduction

Solar cell attracts more and more attentions recently since it transfers and storages energy directly from the sun light without consuming natural resources on the earth and polluting environment. In 2002, the solar industry delivered more than 500 MW per year of photovoltaic generators. More than 85% of the current production involved crystalline silicon technologies. These technologies still have a high cost reduction potential, but this will be limited by the silicon feedstock (Diehl et al., 2005; Lee et al., 2004). On the other hand the so-called second generation thin film solar cells based on a-Si, μc-Si, Cu(In,Ga)(Se,S)2, rare earth or CdTe have been explored(Shah et al.,2005; Li et al.,2004). Crystalline silicon on glass (CSG) solar cell technology was recently developed by depositing silicon film on a glass substrate with an interlayer. It can addresses the difficulty that silicon wafer-based technology has in reaching the very low costs required for large-scale photovoltaic applications as well as the perceived fundamental difficulties with other thin-film technologies (M. A. Green et al., 2004). This technology combines the advantages of standard silicon wafer-based technology, namely ruggedness, durability, good electronic properties and environmental soundness with the advantages of thin-films, specifically low material use, large monolithic construction and a desirable glass substrate configuration.
This Chapter will descript research about the polycrystalline silicon thin film absorber based on CSG technology with high efficiency. Line shaped electron beam recrystallized polycrystalline silicon films of a 20μm thickness deposited on the low cost borosilicate glass-substrate, which are the base for a solar cell absorber with high efficiency and throughput. It is known that the morphology of polycrystalline silicon film and grain boundaries have strong impact on the photoelectric transformation efficiency in the later cell system. Thus, this study concentrates on the influence of recrystallization on the silicon-contact interface and the surface morphology.

2. Experiment methods

Fig. 1 shows the schematic illustration of the silicon solar cell used in this work. The substrate of polycrystalline silicon thin film is Borosilicate glass, which is 10×10×0.07cm^3 in size. A pure tungsten layer of 1.2μm was sputtered on the glass substrate at DC of 500W in

an argon atmosphere, which has almost the same thermal expansion coefficient of $4.5\times10^{-6}K^{-1}$ as that of the silicon film (Linke et al., 2004; Goesmann et al., 1995). This tungsten interlayer was used as a thermal and mechanical supporting layer for deposition of the silicon film. Nanocrystalline silicon films were then deposited on the tungsten interlayer by the plasma enhanced chemical vapour deposition process (PECVD) within $SiHCl_3$ and H_2 atmosphere. Details of the process were described in References (Rostalsky et al., 2001; Gromball et al., 2004, 2005). The power density used was $2.5W/cm^2$. The gap in the PECVD parallel plate reactor was 10mm and the substrate temperature was 550℃. The flow rate $H_2/SiHCl_3$ is 0.25 to reduce the hydrogen and chlorine content in the film. Boron trichloride (BCl_3) was added in the gas for an in-situ p-doping. The process pressure was chosen to 350 Pa for the minimized stress. At the above conditions, the deposition rate up to 200nm/min was obtained. After a silicon film of 15-20µm thickness was deposited, a SiO_2 layer of 400nm thickness was deposited on the top of the silicon from $SiHCl_3$ and N_2O within 5 min to prevent balling up.

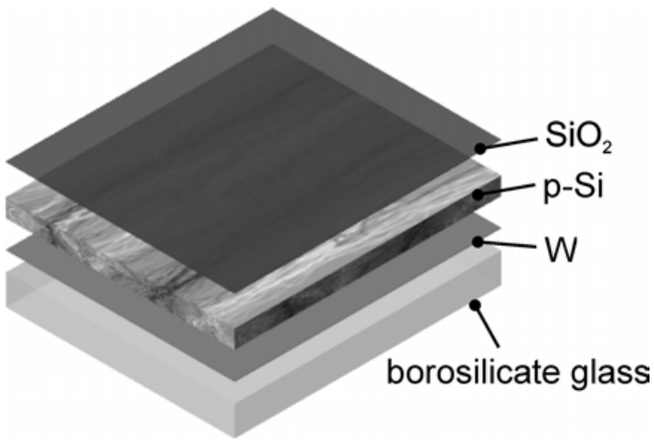

Fig. 1. Structure of thin film silicon solar cell

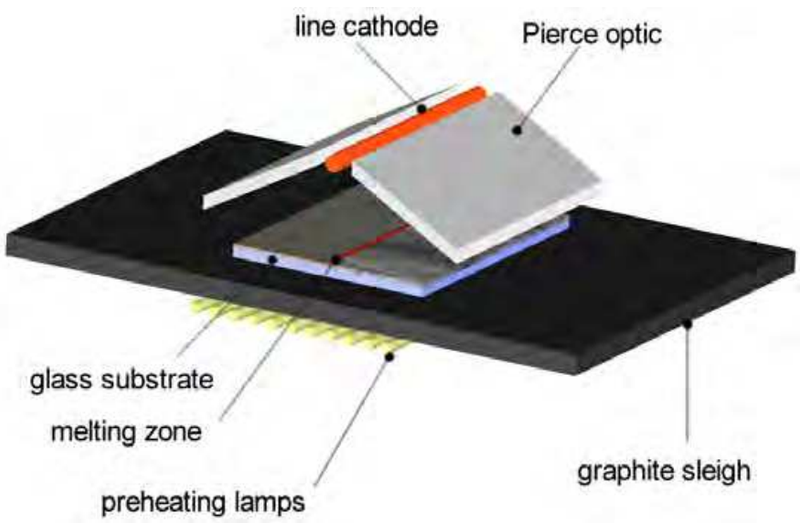

Fig. 2. Schematic of the linear electron beam recrystallization system (Gromball et al., 2005)

The P-doped polycrystalline silicon absorber of 10cm² was melted and recrystallized by a controlled line shaped electron beam (size in 1×100mm²) as described in Fig.2. The appearance of the sample after recrystallization was shown in Fig.3. The samples are preheated from the backside to 500°C within 2 min by halogen lamps. The electron beam energy density applies to the films is a function of the emission current density, the accelerating voltage and the scan speed. The scan speed is chosen to 8mm/s and the applied energy density changes between 0.34J/mm² and 0.4J/mm². To obtain the required grain size, the silicon should be melted and re-crystallized. Therefore, temperature in the electron beam radiation region should be was over the melting point of silicon of 1414°C. The surface morphology of the film, as well as distribution of WSi_2 phase under different energy densities has been investigated by means of a LEO-32 Scanning Electron Microscopy.

Fig. 3. Appearance of polycrystalline silicon absorber after recrystallization

3. Results and discussion

3.1 Microstructure of the capping layer

The applied recrystallization energy density strongly influences the surface morphology and microstructure of the recrystallized silicon film. With the energy increasing, the capping layer becomes smooth and continuous and less and small pinholes form in the silicon film. Excess of recrystallization energy density leads to larger voids in the capping layer, more WSi_2/Si eutectic crystallites, a thinner tungsten layer and a thicker tungstendisilicide layer.
Fig.4 gives the top view of the polycrystalline silicon film after the recrystallization. The EB surface treatment leads to recrystallization to obtain poly-Si films with grain sizes in the order of several 10μm in width and 100μm in the scanning direction as shown in Fig.5. The polycrystalline silicon films in Fig.4 are EB remelting with four different EB energy densities. Area A was treated with an energy density of 0.34J/mm² (the lowest of the four areas) while area D was treated with an energy density of 0.4J/mm² (highest of the four areas) on the same nanocrystalline silicon layer.

Fig. 4. Top view of the recrystallized silicon film, with increase of applied energy density from the left to the right

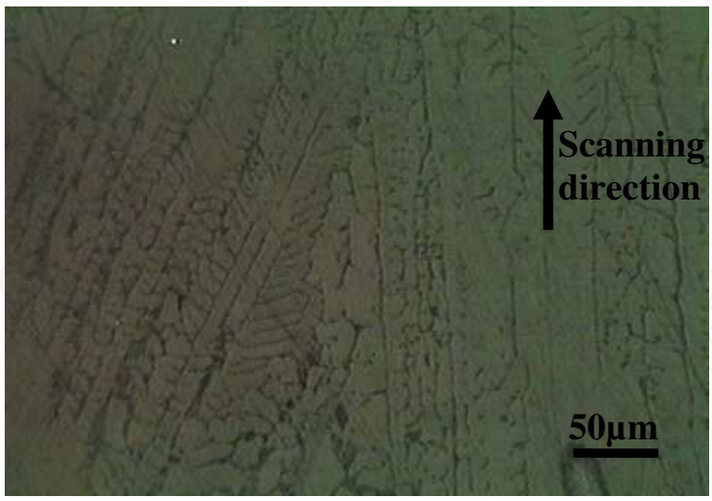

Fig. 5. Grain microstructure of Ploy-Silicon absorber after recrystallization

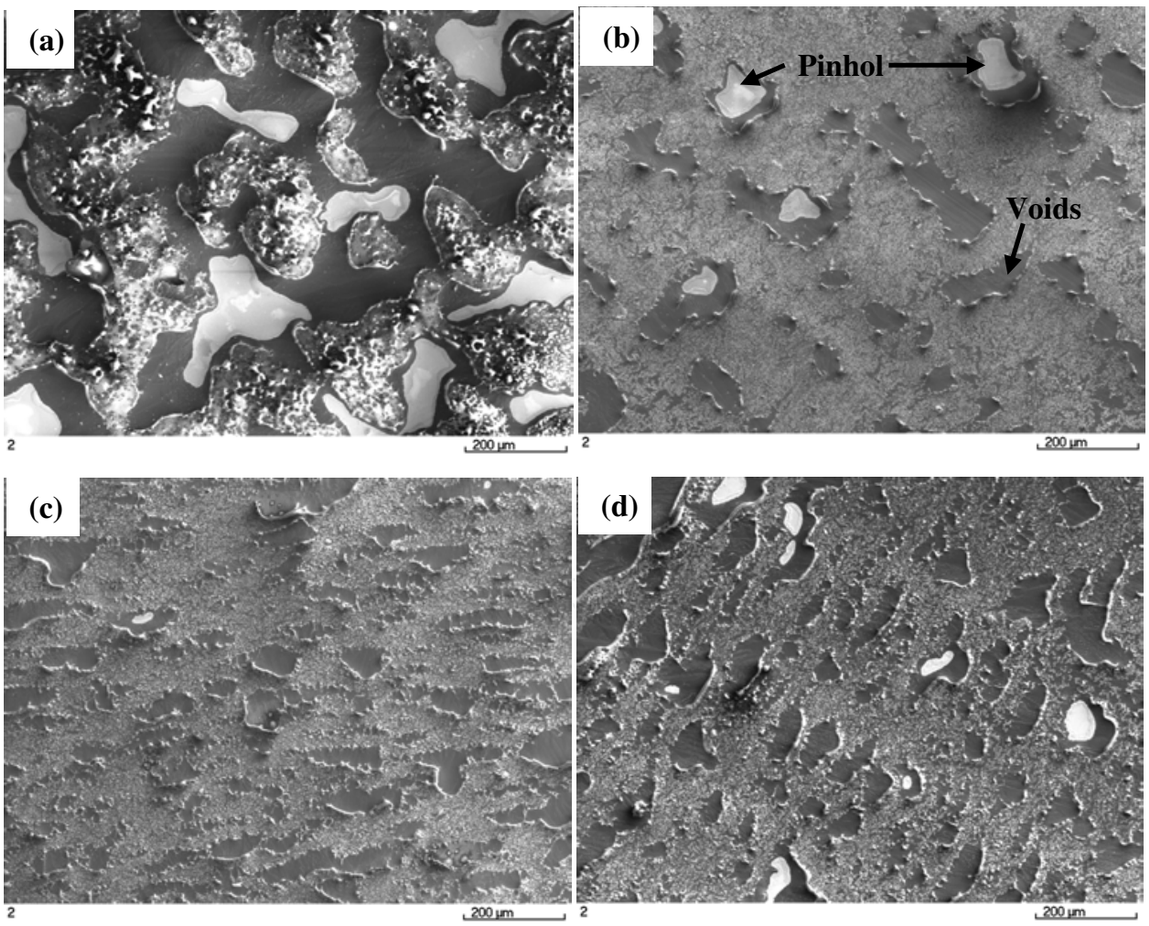

(a) ϵ=0.34J/mm2 ; (b) ϵ=0.36J/mm2 ; (c) ϵ=0.38J/mm2; (d) ϵ=0.4J/mm2

Fig. 6. Surface morphology of the recrystallized silicon layer under different energy density ϵ (Fu et al., 2007)

Fig.6 and Fig.7 show the morphology and microstructure of the EB treated layers. The nanocrystalline silicon is zone melted and recrystallized (ZMR) completely under all the energy chosen in this experiment. It can be seen that after the EB surface treatment, micro-sized silicon grains were formed in all the samples treated under different electron beam energy density ϵ.

The outmost surface was silicon dioxides with some voids and pinholes (bright spots), as shown in Fig.6. Large areas with a rough surface were where the silicon dioxide capping layer (SiO_2) existed. The voids (the dark area in Fig.6) in the silicon dioxide capping layer penetrated into the silicon layer with smooth edges. The bright areas were the bottom of the pinholes in which the WSi_2 remained.

Influences of the EB energy density on the morphology of deposited films are summarized in Table 1. The energy density influences the surface morphology of the film system strongly. The capping layer exhibited more voids when a lower EB energy density was used, as shown in Fig.6a. The SiO_2 capping layer is rougher and appeared as discontinuous droplet morphology in this condition. In addition, large tungstendisilicide pinholes formed due to the lower fluidity and less reaction between the silicon melt and the tungsten interlayer. When the EB energy density was increased, the capping layer becomes smoother and the size of voids was reduced. The number and size of pinholes also became smaller. However, when excess EB energy was applied, the solidification process became unstable and the amount of pinholes increased again. The silicon dioxide capping layer became discontinuous in this case, as shown in Fig. 6d.

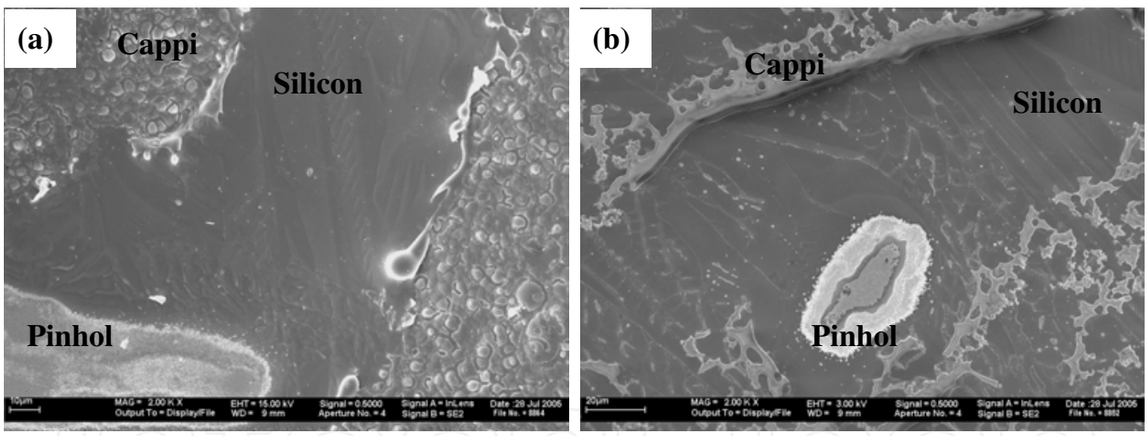

(a) ϵ=0.34J/mm² ; (b) ϵ=0.4J/mm²

Fig. 7. Microstructure of the capping layer and silicon grain under different energy density ϵ (Fu et al., 2007)

It was suggested that the voids are caused by the volume change of the capping layer and the silicon melt during the recrystallization process. Early work [6] suggested that the silicon dioxide in the capping layer could be considered as a fluid with a relatively high viscosity at the EB treatment temperature. For the same amount of silicon, the volume of the solid V_S is about 1.1 times of that of the liquid V_L. Therefore, during solidification process of the silicon melt, the volume increases will produce a curved melt surface. This will generates a tensile stress in the capping layer because of he interface enlargement between the viscous capping layer and the molten silicon. Once the critical strain of the capping layer is surpassed, voids will form in the capping layer. Due to the surface tension of the capping layer and its

adhesion to the silicon melt the capping layer also arches upwards and widens the voids. This effect is enhanced by thermal stress and outgassing during the solidification process [5]. As the size, area and viscosity of the SiO_2 layer is affected by the EB energy density, the size and the number of the voids in the capping layer are dependant on the EB energy density as well.

Energy level	SiO_2 capping/ voids	pinholes	$W_{remaining}$/ WSi_2 ratio	WSi_2/Si eutectic
Low (0.34J/mm²)	rough, droplet morphology	High density, biggest (>200µm)	21.7%	fine
Middle (0.36-0.38J/mm²)	smooth, continuous	sporadic, small size (<50µm)	13.3%	coarse
High (0.4J/mm²)	smooth, discontinuous	Low density, bigger(<100µm)	10.5%	coarser and widely spread

Table 1. Influence of the recrystallization energy on the surface morphology of the silicon film system

3.2 Formation of eutectic (WSi_2/Si)

This Chapter gives the details about the formation of Tungstendisilicide (WSi_2). The film system consists of a 20µm thick silicon layer on a 1.2µm thick tungsten film. Tungstendisilicide (WSi_2) is formed at the interface tungsten/silicon but also at the grain boundaries of the silicon. Because of the fast melting and cooling of the silicon film, the solidification process of the silicon film is a nonequilibrium solidification process.

It was claimed that tungstendisilicides were formed in their tetragonal (Hansen, 1958; Döscher et al., 1994) by the solid/solid state reaction and the solid/liquid state reaction between tungsten and silicon according to equation (1) and (2).

$$2Si_{(s)} + W_{(s)} \xrightarrow{700°C-1390°C} WSi_{2(s)} \tag{1}$$

$$2Si_{(l)} + W_{(s)} \xrightarrow{>1390°C} WSi_{2(s)} \tag{2}$$

Formation of the eutectics can be explained using the phase diagram of the Si-W alloy system, as shown in Fig.8. The reactions should start at temperatures above 700°C. The eutectic crystallites (WSi_2/Si) are precipitated from the silicon melt at a eutectic concentration of 0.8 at% W at the eutectic temperature 1390°C in thermal equilibrium. With the temperature increased to above the eutectic temperature (1390°C) for tungsten enriched silicon melt, the WSi_2 layer mainly formed through a solid-liquid reaction and the thickness of the silicide layer increased rapidly. Because 100ms (the FWHM of the electron beam related to the scan speed) were sufficient to generate the tungstendisilicide layer. However, in this experiment, the solidification process of the nanocrystalline silicon was completed within 12.5 seconds for a sample of 10cm² area. Therefore, the solidification process was completed in a nonequilibrium state and the liquid-solid transformation line will divert from equilibrium line shown in Fig.8. At the beginning of the silicon solidification, the formation of tungstendisilicide crystallites will be suppressed by the rapid freezing and followed by the formation of solid silicon. These crystallites start to form just below the

liquid-solid transformation temperature, and their growth will be not immediately accompanied by the tungstendisilicide crystallite formation. Therefore, the silicon phase forms dendrites, which grow over a range of temperature like ordinary primary crystallites. Below the eutectic reaction temperature, the remaining melt solidifies eutectically as soon as the melt is undercooled to a critical temperature to allow silicon crystallite growth.

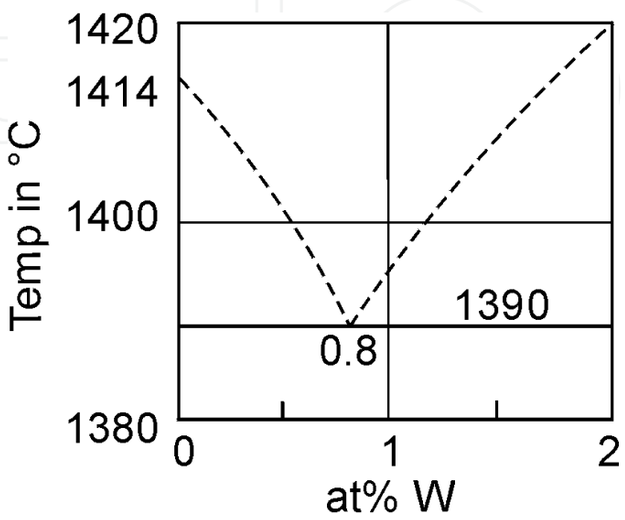

Fig. 8. Phase diagram of the Si-W alloy system in equilibrium (Hansen, 1958)

3.3 Microstructure and distribution of the eutectic crystallites (WSi2/Si) under different recrystallization energy

Tungstendisilicide (WSi_2) was formed at the tungsten/silicon interface but also at the grain boundaries of the silicon throughout all the EB energy density range. A top view scanning electron spectroscopy (SEM) and EDX analysis of the surface region showed that eutectic structure (tungstendisilicide precipitates / silicon) were mainly localized at the recrystallized silicon grain boundaries, as is shown in Fig.9. A typical hypoeutectic structure was found in the exposed silicon layer, which consisted of cored primary silicon dendrites (dendritic characteristic was not very evident) surrounded by the eutectic of the silicon and the tungstendisilicide precipitates. In this eutectic, tungstendisilicide (white areas in the lamellar shape) grew until the surrounding silicon melt had fully crystallized. The eutectic statistically distributed at the primary silicon grain boundaries. The formation and distribution of the eutectic depended on the crystallization and the growth dynamic of the tungsten enriched silicon melt. This is a nonequilibrium solidification process.

The size and the amount of the tungstendisilicide/silicon eutectic depended on the course of the process: when the higher the energy was used in the recrystallization process of the silicon layer, more and large tungstendisilicide crystals grew in the silicon melt. In addition, the WSi2/Si eutectic became coarser at the primary silicon grain boundaries and spread more widely. This was due to the prolonged solidification period for the tungsten enriched silicon melt in the remaining liquid, primarily at the grain boundary. At these sites, the tungstendisilicide crystallites precipitated in the final solidification areas at lower temperature than in case of equilibrium, due to the high tungsten concentration in the

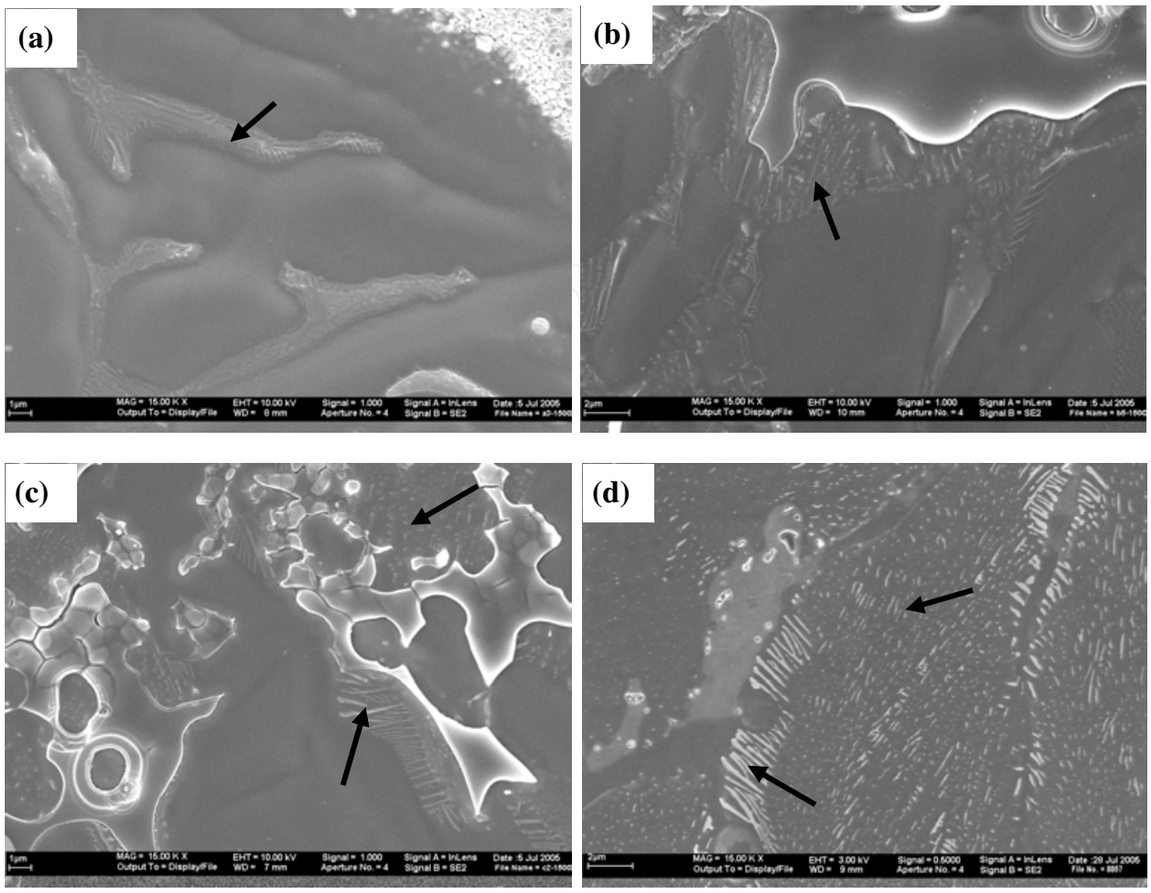

(a) ϵ=0.34J/mm²; (b) ϵ=0.36J/mm²; (c) ϵ=0.38J/mm²; (d) ϵ=0.4J/mm²

Fig. 9. SEM results of the eutectic structure under different recrystallization energy density ϵ (Fu et al., 2007)

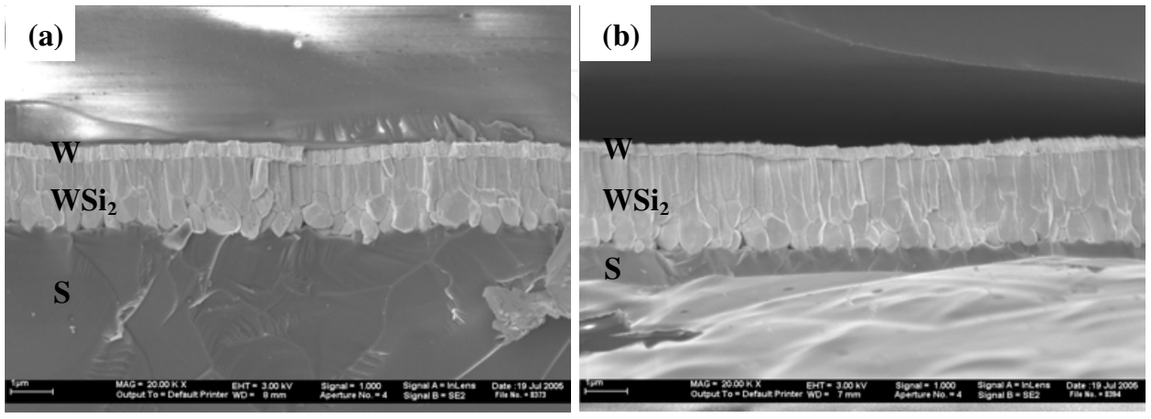

(a) ϵ=0.34J/mm² ; (b) ϵ=0.40J/mm²

Fig. 10. Cross section of typical silicon film system under different energy density ϵ (Fu et al., 2007)

volume. For high EB energy density there was more time for the precipitation and growth of tungstendisilicide and thus more tungstendisilicide crystallites were precipitated at the silicon grain boundaries. The strong tendency of formation of tungstendisilicide at the primary grain boundaries would reduce the efficiency of the solar absorber. Thus a high energy density is not favorable for the recrystallization process.

Fig.10 shows the cross section of a typical resolidified silicon film remelted with different EB energy densities. Tungstendisilicides (WSi_2) were formed in the region between the tungsten layer and the silicon layer without relationship to the EB energy density range applied in this research. A thick tungstendisilicide of 2.0-2.86μm exhibited in this experiment. The higher the applied EB energy density, the thicker the tungstendisilicide layer between the tungsten and the silicon layer, the thinner the remaining tungsten layer will be.

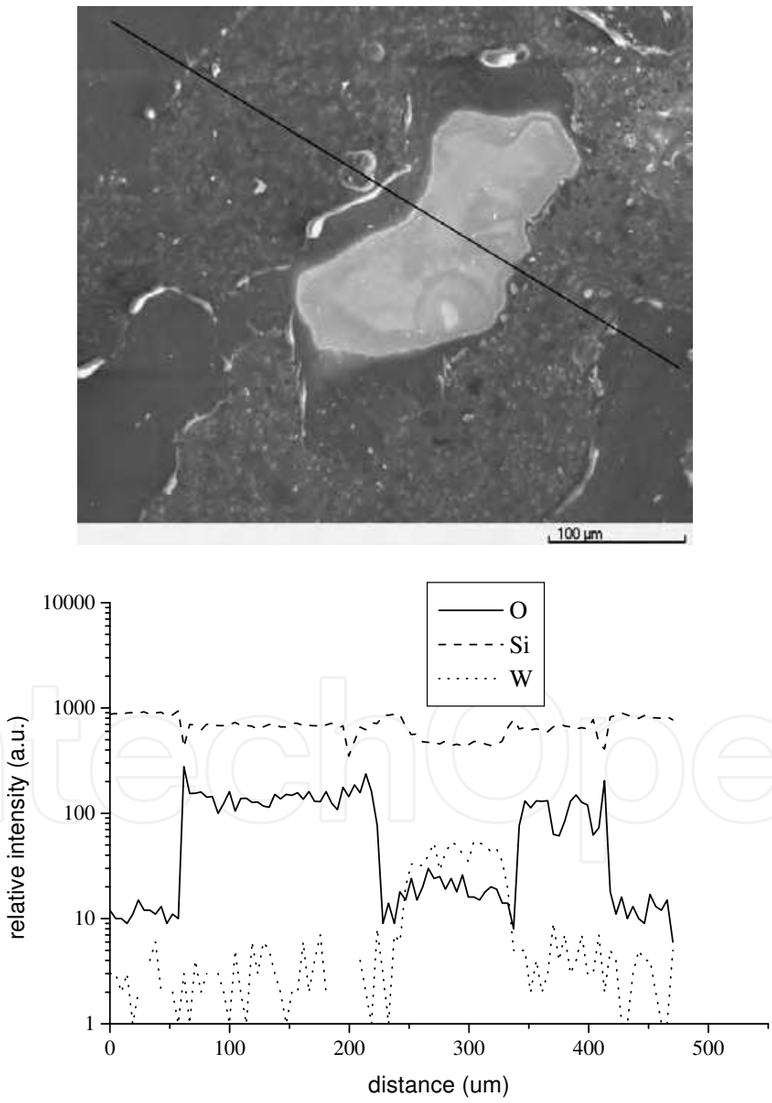

Fig. 11. SEM top view of the recrystallized silicon film in the pinhole area and its EDX line profile mapping results

3.4 Impurities in the recrystallized silicon film

The relatively high chlorine and hydrogen concentrations in the order of 0.5at% lead to outgassing during the recrystallization in completely melting regimes. This effect makes the capping layer arch upwards and widens the voids. Isolated pinholes in the silicon film can be observed. A weak hydrogen chloride peak is detected by mass spectrometry in the base gas atmosphere of the recrystallization chamber. Fig.11 shows an area surrounding a pinhole taken with SEM and the relative element concentrations measured by energy dispersive x-ray analysis (EDX) along the black line. There are no chlorine and hydrogen in the area surrounding a pinhole in the recrystallized film.

4. Summary

This Chapter descried the influence of the applied EB energy density used for the recrystallization process on the surface morphology of the ploy-silicon film system. At a low EB energy density, the voids were formed in the capping layer and the SiO_2 capping layer exhibited a rougher and droplet morphology. With the increase of EB energy density, the capping layer became smooth and the size of the voids decreased. The size and amount of pinholes increased again if the EB energy density was too high. This also led to the formation of larger voids in the capping layer as well as coarser and wider spreading of a WSi_2/Si eutectic crystallite at the grain boundaries.

This Chapter also gave the details about the formation of Tungstendisilicide (WSi_2). The tungstendisilicide precipitates/silicon eutectic structures were mainly localized in at the tungsten/silicon interface but also at the grain boundaries of the silicon throughout all the EB energy density range, as well as the relationship between energy density and microstructure of WSi_2/W areas. Tungstendisilicide forms in its tetragonal by the reaction of tungsten with silicon. WSi_2 improves the wetting and adhesion of the silicon melt but the tungsten layer may degrade the electrical properties of the solar absorber. The formation and distribution of the eutectic depended on the crystallization and the growth dynamic of the tungsten enriched silicon melt. This is a nonequilibrium solidification process.

A tungstendisilicide layer was formed between the tungsten layer and the silicon layer for all EB energy densities used. The higher the applied EB energy density, the thicker the tungstendisilicide layer grows and the thinner the tungsten layer left. It is important to perform the recrystallization process at a moderate energy density to suppress the formation of both WSi_2/Si eutectic and pinholes. In addition, there are no chlorine and hydrogen in the area surrounding a pinhole after recrystallization because of outgassing during the solidification.

5. Acknowledgements

The author would like to thank Prof. J. Müller and Dr. F. Gromball of Technische Universit.t Hamburg-Harburg in Germany for providing experimental conditions and interesting discussion, and also remember Prof. J. Müller with affection for his human and scientific talents. This research was financially supported by the German Federal Ministry for the Environment, Nature Conservation and Nuclear Safety under contract #0329571B in collaboration with the Hahn Meitner Institute (HMI), Berlin-Adlershof, Department for Solar Energy Research. The author was financially supported by China Scholarship Council

(CSC) and the Research Fund of the State Key Laboratory of Solidification Processing (NWPU), China (Grant No. 78-QP-2011).

6. References

Diehl W., Sittinger V. & Szyszka B. (2005). Thin film solar cell technology in Germany. *Surface and Coatings Technology*, Vol.193, No. 1-3, (April 2005), pp.329-334, ISSN: 0257-8972

Döscher M., Pauli M. and Müller J. (1994). A study on WSi_2 thin films, formed by the reaction of tungsten with solid or liquid silicon by rapid thermal annealing. *Thin Solid Films*, Vol.239, No. 2, (March 1994), pp.251-258, ISSN: 0040-6090

Dutartre D. (1989). Mechanics of the silica cap during zone melting of Si films. *Journal of Apply Physics*, Vol.66, No. 3, (August 1989), pp.1388-1391, ISSN: 0021-8979

Fu L., Gromball F., Groth C., Ong K., Linke N. & Müller J. (2007). Influence of the energy density on the structure and morphology of polycrystalline silicon films treated with electron beam. *Materials Science and Engineering B*, Vol.136, No. 1, (January 2007), pp.87–91, ISSN: 0921-5107

Green M. A., Basore P. A., Chang N., Clugston D., Egan R., Evans R. Hogg D., Jarnason S., Keevers M., Lasswell P., O'Sullivan J., Schubert U., Turner A., Wenham S. R. & Young T. (2004). Crystalline silicon on glass (CSG) thin-film solar cell modules. *Solar Energy*. Vol.77, No. 6, (December 2004) , pp.857-863, ISSN: 0038-092X

Goesmann F. & Schmid-Fetzer R. (1995). Stability of W as electrical contact on 6H-SiC: phase relations and interface reactions in the ternary system W-Si-C. *Materials Science and Engineering B*, Vol. 34, No. 2-3, (November 1995), pp.224-231, ISSN: 0921-5107

Gromball F., Heemeier J., Linke N., Burchert M. & Müller J. (2004). High rate deposition and in situ doping of silicon films for solar cells on glass. *Solar Energy Materials & Solar Cells*, Vol.84, No. 1-4, (October 2004), pp.71-82, ISSN: 0927-0248

Gromball F., Ong K., Groth C., Fu L., Müller J., Strub E., Bohne W. & Röhrich J. (2005). Impurities in electron beam recryatallised silicon absorbers on glass, *Proceedings of 20th European Photovoltaic Solar Energy Conference and Exhibition*, Barcelona, Span, July, 2005.

Hansen M. (1958). Constitution of binary alloys, In: *Metallurgy and Metallurgical Engineering Series*, Kurt Anderko, pp.100-1324, McGraw-Hill Book Company, ISBN-13: 978-0931690181, ISBN-10: 0931690188, London

Lee G. H., Rhee C. K. & Lim K. S. (2006). A study on the fabrication of polycrystalline Si wafer by direct casting for solar cell substrate. *Solar Energy*, Vol.80, No. 2, (February 2006), pp.220-225, ISSN: 0038-092X

Li B. J., Zhang C. H. & Yang T. (2005). *Journal of Rare Earths*. Vol.23, No. 2, (April 2005), pp.228-230, ISSN: 1002-0721

Linke N., Gromball F., Heemeier J. & Mueller J. (2004). Tungsten silicide as supporting layer for electron beam recryatallised silicon solar cells on glass, *Proceedings of 19th European Photovoltaic Solar Energy Conference and Exhibition*, Paris, France, July, 2004.

Rostalsky M. & Mueller J. (2001). High rate deposition and electron beam recrystallization of silicon films for solar cells. *Thin Solid Films*, Vol.401, No. 1-2, (December 2001), pp.84-87, ISSN: 0040-6090

Shah A. V., Schade H., Vanecek M., Meier J., Vallat-Sauvain E., Wyrsch N., Kroll U., Droz C. & Bailat J. (2004). Thin-film silicon solar cell technology. *Progress in Photovoltaics: Research and Applications*. Vol.12, No. 2-3, (March 2004), pp.113-142, ISSN: 1099-159X

IntechOpen

IntechOpen

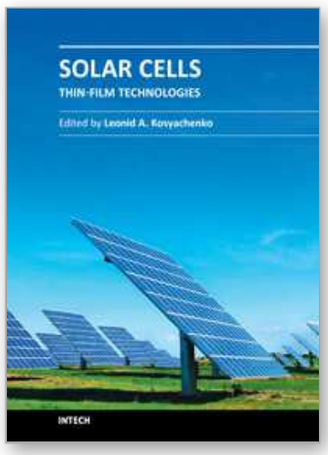

Solar Cells - Thin-Film Technologies

Edited by Prof. Leonid A. Kosyachenko

ISBN 978-953-307-570-9
Hard cover, 456 pages
Publisher InTech
Published online 02, November, 2011
Published in print edition November, 2011

The first book of this four-volume edition is dedicated to one of the most promising areas of photovoltaics, which has already reached a large-scale production of the second-generation thin-film solar modules and has resulted in building the powerful solar plants in several countries around the world. Thin-film technologies using direct-gap semiconductors such as CIGS and CdTe offer the lowest manufacturing costs and are becoming more prevalent in the industry allowing to improve manufacturability of the production at significantly larger scales than for wafer or ribbon Si modules. It is only a matter of time before thin films like CIGS and CdTe will replace wafer-based silicon solar cells as the dominant photovoltaic technology. Photoelectric efficiency of thin-film solar modules is still far from the theoretical limit. The scientific and technological problems of increasing this key parameter of the solar cell are discussed in several chapters of this volume.

How to reference

In order to correctly reference this scholarly work, feel free to copy and paste the following:

L. Fu (2011). Application of Electron Beam Treatment in Polycrystalline Silicon Films Manufacture for Solar Cell, Solar Cells - Thin-Film Technologies, Prof. Leonid A. Kosyachenko (Ed.), ISBN: 978-953-307-570-9, InTech, Available from: http://www.intechopen.com/books/solar-cells-thin-film-technologies/application-of-electron-beam-treatment-in-polycrystalline-silicon-films-manufacture-for-solar-cell

INTECH
open science | open minds

InTech Europe
University Campus STeP Ri
Slavka Krautzeka 83/A
51000 Rijeka, Croatia
Phone: +385 (51) 770 447
Fax: +385 (51) 686 166
www.intechopen.com

InTech China
Unit 405, Office Block, Hotel Equatorial Shanghai
No.65, Yan An Road (West), Shanghai, 200040, China
中国上海市延安西路65号上海国际贵都大饭店办公楼405单元
Phone: +86-21-62489820
Fax: +86-21-62489821

© 2011 The Author(s). Licensee IntechOpen. This is an open access article distributed under the terms of the Creative Commons Attribution 3.0 License, which permits unrestricted use, distribution, and reproduction in any medium, provided the original work is properly cited.

IntechOpen

IntechOpen